

A Class of Interstellar OH Masers Associated with Protostellar Outflows

Alice L. Argon and Mark J. Reid

Harvard-Smithsonian Center for Astrophysics, 60 Garden Street/MS42, Cambridge MA 02138

Karl M. Menten

Max-Planck-Institut für Radioastronomie, Auf dem Hügel, D-53121 Bonn, Germany

ABSTRACT

Using the Very Large Array, we have detected weak OH maser emission near the Turner–Welch protostellar source in the W3 OH region. Unlike typical interstellar OH masers, which are associated with ultra-compact HII regions, our measured positions and proper motions (from Very Long Baseline Interferometry) indicate that these OH masers are associated with a bipolar outflow traced by strong H₂O masers. These OH masers may be part of a class of interstellar OH masers that are associated with very young stars which have yet to, or may never, create ultra-compact HII regions. This class of OH masers appears to form near the edges of very dense material (within which H₂O masers form), where total densities drop precipitously and interstellar UV radiation is sufficient to dissociate the H₂O molecules. Observations of this class of OH masers may be an important way to probe the distribution of this important molecule in interstellar shocks at arcsecond resolution or better.

Subject headings: ISM: individual (W3)—ISM: jets and outflows—masers—radiation mechanisms: nonthermal—radio lines: ISM—stars: formation

1. Introduction

In the Milky Way, hydroxyl masers (OH) are found associated with either evolved stars (stellar masers), regions of massive star formation (interstellar masers), or the interface between SNRs and molecular material. Interstellar OH masers are often observed from molecular material surrounding ultra-compact HII (UCHII) regions. The OH masers in the source W3 OH are some of the strongest and best studied of their kind. In this source, the

OH maser spots have been mapped with VLBI observations and found projected toward an UCHII region (Reid et al. 1980). Proper motions of these masers (Bloemhof, Reid, & Moran 1992) suggest a slow, general expansion with a velocity of a few km s^{-1} .

Interstellar H_2O masers are often found in the same star forming regions as OH masers. However, frequently the H_2O masers do not appear to be *directly* associated with UCHII regions. In fact, rarely can one detect a stellar source at the center of the H_2O maser flow, not even at IR wavelengths, suggesting a deeply embedded and probably very young object. Moreover, H_2O masers are also found in regions of low-mass star formation, which are devoid of OH masers. H_2O masers often exhibit strong outflow motions, with expansion speeds $\sim 30 \text{ km s}^{-1}$, and sometimes high velocity features moving at hundreds of km s^{-1} .

In this paper we present a detailed analysis of weak OH masers in the W3 OH region that do *not* appear to be associated with an UCHII region. Instead they seem to form at the edges of the outflow from the Turner–Welch object (Turner & Welch 1984), a protostellar source or cluster of sources (Wyrowski, Schilke, Walmsley, & Menten 1999) that drives the H_2O masers near W3 OH (Alcolea, Menten, Moran, & Reid 1993) and a synchrotron jet (Reid et al. 1995; Wilner, Reid, & Menten 1999). Our observations suggest that protostellar outflows may be an important mechanism for the production of weak OH masers when no ionizing stars are present.

2. Observations and Results

2.1. VLA Observations and Results

W3 OH was observed in the 1612.231, 1665.4018, 1667.359, and 1720.530 MHz OH transitions with the NRAO¹ Very Large Array (VLA) on 1992 December 27 using all 27 antennas in the A-configuration. Three 1.5 minute scans were obtained in the 1665 transition, three 2.5 minute scans in the 1667 transition, and one 2.5 minute scan in each of the remaining two transitions. When a transition was observed more than once, scans were spread over about 3 hours. Weather conditions were excellent.

Observations were made in both left-circular (LCP) and right-circular (RCP) polarizations. These observations were part of a project to map a large sample of interstellar OH masers (Argon, Reid, & Menten 2000). The observing bandwidth of 0.1953 MHz was cen-

¹The National Radio Astronomy Observatory (NRAO) is operated by Associated Universities, Inc., under a cooperative agreement with the National Science Foundation.

tered at an LSR velocity of -44.0 km s^{-1} . For each band the inner 128 spectral channels (out of a total of 256) were correlated, yielding a channel separation of 0.14 km s^{-1} .

Calibration and imaging were done in the Astronomical Image Processing System (AIPS). Channel “0” observations (an average of the central 75% of each bandpass) were used to calibrate the complex instrumental gain for each antenna. We employed the standard method of boot-strapping the flux density of a (variable) secondary calibrator, B0212+735, from the flux density of the primary calibrator, 3C 286. We then determined complex gains for the secondary calibrator using the AIPS task CALIB, interpolated those gains to the W3 OH observation times with the task CLCAL, and applied them to the full spectral-line database with the tasks TACOP and SPLIT. Observations of the secondary calibrator were made immediately before and after each W3 OH scan to ensure accurate interpolation.

To remove the effects of any residual atmospheric phase corruption, we “self-calibrated” the data. This was accomplished by selecting a strong unresolved feature in one of the polarizations for each transition (called the “reference feature”), shifting the interferometer phase center to the position of that feature, determining residual phases using a point source, and subtracting those residual phases from the data in all spectral channels in both polarizations. The reference features chosen were the $v_{LSR} = -48.9 \text{ km s}^{-1}$ and -44.4 km s^{-1} channels at 1665 and 1667 MHz, respectively, both in LCP.

A comparison of the positions of the strong OH masers in our study (Argon, Reid, & Menten 2000) and another study (Bloemhof, Reid, & Moran (1992) and references therein), taking into account the different map center locations, suggests that our absolute position error for the 1665 MHz transition is $\approx 0.^{\prime\prime}1$ in each direction. Self-calibration was followed by imaging, whereby each spectral channel was mapped and CLEANed. We searched an area of $128'' \times 128''$ (512×512 pixels). Note that because our sources can be 100% circularly polarized, we divided the maps produced by MX by a factor of two so that Stokes I is obtained by summing (rather than averaging) the RCP and LCP maps.

After imaging, selected peaks were fit with a two-dimensional Gaussian brightness distribution to determine their flux density, size, and offset from the reference feature. While strong OH maser emission for the UCHII region has been mapped before, we searched for emission beyond the innermost $5'' \times 5''$. Spurious maser features were rejected by demanding that the following four constraints be met:

- 1) Peaks had to have a flux density of at least 4.5 times the channel rms noise. Typical channel rms noise levels were 28 mJy for the 1665.4018 MHz transition and 26 mJy for the 1667.359 MHz transition.
- 2) Peaks had to have a flux density of at least 1.3 times the absolute value of the largest

negative peak in the channel map.

- 3) Peaks could not be any weaker than 1/150 of the peak in the map owing to dynamic range limitations, which are particularly severe at 1665 MHz because of the strong OH emission from the UCHII region between $-43 < v_{LSR} < -47$ km s $^{-1}$. Two “peaks” appear in the spectrum shown in Figure 1 that do not satisfy this criterion. They are artifacts of a 132 Jy (-46.3 km s $^{-1}$, LCP) and a 201 Jy (-45.0 km s $^{-1}$, RCP) feature.
- 4) Peaks had to persist over three or more adjacent channels to within a synthesized beam width.

We found two spots of OH maser emission satisfying all four criteria, one at 1665 and the other at 1667 MHz (see Table 1). Since the expected uncertainty for a point source is approximately half the synthesized beam (1'') divided by the signal-to-noise ratio, the relative position error in each coordinate is $\approx 0.^{\prime\prime}06$ and $\approx 0.^{\prime\prime}07$ for the 1665 and 1667 MHz transitions, respectively. Spectra of the two features at the pixel of their maximum flux density are shown in Figure 1. Both features are $\gtrsim 8\sigma$ detections and were detected by Gaume & Mutel (1987), who, while noting that they were in the vicinity of the water masers and HCN emission, did not discuss their significance. Our -42.4 and -49.3 km s $^{-1}$ features were reported at -42.8 and -48.3 km s $^{-1}$, respectively, by Gaume & Mutel, who list velocities of the peak channel emission in 1.1 km s $^{-1}$ wide channels. Thus, the agreement in both position and velocity for these two measurements is reasonable. Gaume & Mutel also observed one additional spot of weak emission (0.1 Jy, a 3σ detection) *outside* of the central 5'' x 5'', that we fail to confirm. Our 1σ noise level was 0.026 Jy in this transition, so if the maser’s flux density was constant (or increasing) in time between their observations in 1985 and ours in 1992, we would have a 4σ detection. Either Gaume & Mutel’s detection is spurious, which is not highly unlikely in a $\sim 10'' \times 10''$ field (containing about 100 independent beams), or the feature weakened over the years.

2.2. VLBI Data and Results

In an attempt to confirm the 1665 MHz VLA detection and obtain a proper motion, we re-mapped the data from two epochs of VLBI observations: one in 1978 by Garcia-Barreto et al. (1988) and the other in 1986 by Bloemhof, Reid, & Moran (1992). (No archival VLBI data for the 1667.359 transition were available). At both epochs, RCP and LCP were observed and there were 96 spectral channels per IF, giving channel separations of 0.12 km s $^{-1}$. Observations were centered at an LSR velocity of -46.0 km s $^{-1}$. At both epochs, we searched for emission within ($\pm 0.^{\prime\prime}1$) of the positions in Table 1. Since the features in

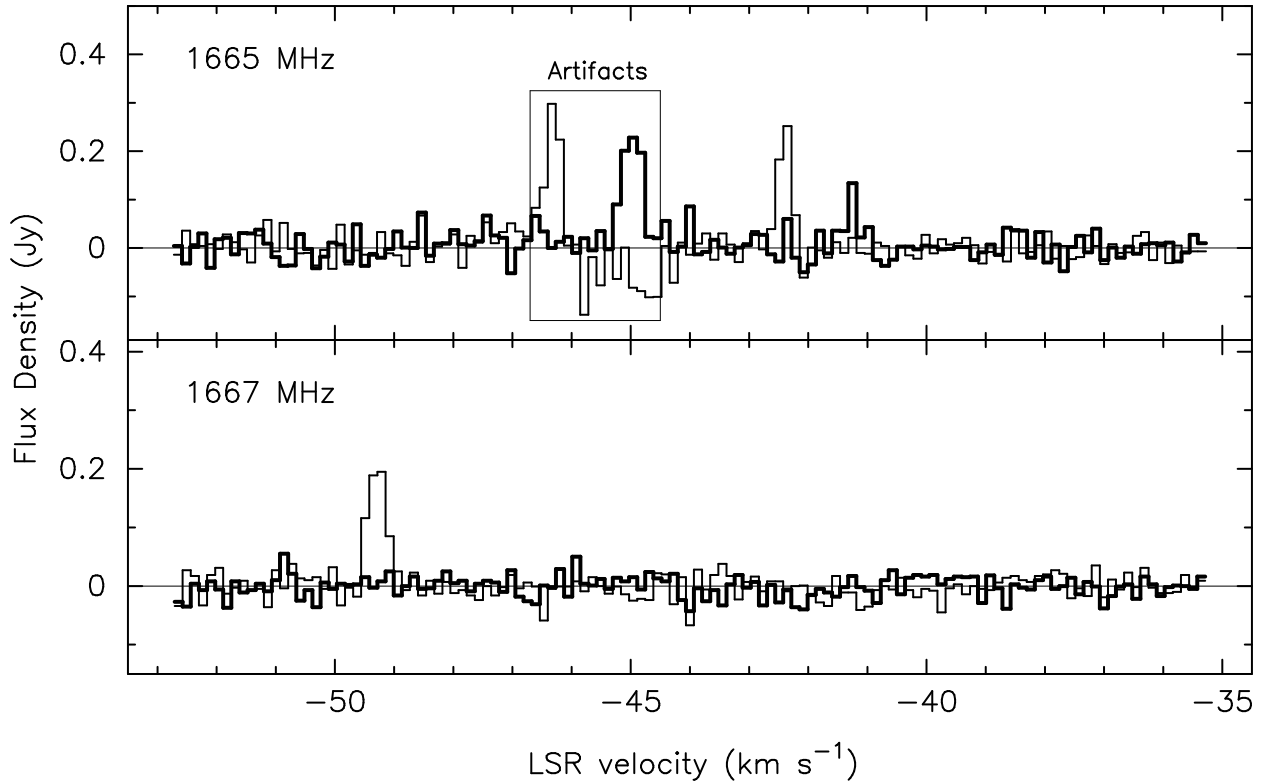


Fig. 1.— Spectra of two “outlying” OH maser features (-42.4 km s^{-1} , LCP at 1665 MHz and -49.3 km s^{-1} , LCP at 1667 MHz) at the positions of their maximum emission. Heavy lines indicate RCP and light lines LCP emission. The “features” at $v_{LSR} = -46.3 \text{ km s}^{-1}$ (LCP) and -45.0 km s^{-1} (RCP) in the 1665 MHz transition are artifacts generated by spatial sidelobes of the strongest 1665 LCP (132 Jy) and RCP (201 Jy) features, respectively, which are located toward the UCHII region. The outlying OH features are *not* artifacts since there is no strong LCP emission at $v_{LSR} = -42.4 \text{ km s}^{-1}$ in 1665 or at -49.3 km s^{-1} in 1667 elsewhere in the map. A 4σ RCP detection at -41.3 km s^{-1} in the 1665 MHz transition may be part of a Zeeman pair, the other member being the -42.4 km s^{-1} feature.

Table 1. VLA Observations of OH Maser Emission^a

Transition (Pol.)	v_{LSR}^b (km s $^{-1}$)	Peak Flux Density ^b (Jy)	Δv^b (km s $^{-1}$)	$\Delta\Theta_x^c$ ($''$)	$\Delta\Theta_y^c$ ($''$)
1665.4018 (LCP)	−42.4	0.25 ± 0.03	0.29	4.17 ± 0.06	-0.09 ± 0.06
1667.359 (LCP)	−49.3	0.20 ± 0.03	0.37	6.81 ± 0.07	-0.06 ± 0.07

Note. — ^a Maser features $> 2.^{\circ}5$ from center of the UCHII region in W3 OH. ^b The quantities v_{LSR} , Δv (FWHM), and peak flux density were determined by fitting a Gaussian profile to the three highest spectral points. ^c Positions are offsets eastward ($\Delta\Theta_x$) and northward ($\Delta\Theta_y$) from the map center of Fig. 2, located at $\alpha_{B1950} = 02^h 23^m 16.^s 499$, $\delta_{B1950} = 61^{\circ} 38' 57.^{\prime\prime}21$, and are weighted averages of the contributing channels. Specifically, the position offsets are relative to the 1665 MHz LCP reference feature at -46.3 km s $^{-1}$ and then shifted by adding $(-0.^{\circ}706, -0.^{\circ}210)$ to the relative maser positions to register them with the map in Fig. 2.

Table 2. VLBI Observations of 1665 MHz LCP OH Maser Emission

Epoch	v_{LSR} (km s $^{-1}$)	Peak Flux Density (Jy)	Δv (km s $^{-1}$)	$\Delta\Theta_x$ ($''$)	$\Delta\Theta_y$ ($''$)
1978	−42.9	0.75 ± 0.10	0.26	4.222 ± 0.001	-0.052 ± 0.001
1986	−42.4	0.17 ± 0.04	0.29	4.199 ± 0.001	-0.094 ± 0.001

Note. — The positional errors are *formal* uncertainties. See text for details and the Table 1 caption for other information.

W3 OH are weak and heavily resolved on long baselines, we used a (u–v)-taper of $20\text{ M}\lambda$. The resulting rms noise levels in the channel maps were about 100 mJy and 35 mJy for 1978 and 1986 observations, respectively.

The VLBI results are given in Table 2 and displayed in Figure 2. The 1665 MHz LCP feature near $v_{LSR} = -42.4\text{ km s}^{-1}$ in our VLA data was found to be present in the 1978 and 1986 VLBI maps, albeit at a slightly different velocity (-42.9 km s^{-1}) in 1978. Note that Gaume & Mutel (1987) report a velocity of -42.8 km s^{-1} for this feature. We registered the maps at the three epochs (two VLBI, one VLA) by using the strongest 1665 MHz LCP feature (132 Jy at -46.3 km s^{-1} in the VLA data), which is located at $\alpha_{B1950} = 02^h23^m16.^s322 \pm 0.^s01, \delta_{B1950} = 61^\circ38'57.^"66 \pm 0.^"1$. The VLBI relative position errors in Table 2 are $\approx 1\text{ mas}$. Assuming these features trace a single cloud of gas, we find a proper motion of about -32 km s^{-1} eastward and -58 km s^{-1} northward, with a *formal uncertainty* of about 2 km s^{-1} in each direction. A distance of 2.2 kpc was assumed. Because the line center velocity of the feature changes by $\approx 0.5\text{ km s}^{-1}$ between the two epochs, a realistic proper motion uncertainty should include the possibility of structural changes in the feature. The span of position offsets over the three or more adjacent channels that comprise a feature is one way to estimate the magnitude of possible structural changes. A typical span was found to be $\approx 2\text{ mas}$, which gives rise to a more *realistic proper motion uncertainty* of $\approx 4\text{ km s}^{-1}$ in each direction. Only the two VLBI epochs were used to estimate the motion since their positional accuracies are far better than the positional accuracy of the VLA epoch. The VLA position, however, is consistent with the derived VLBI motion and our OH motion is consistent with the bipolar outflow seen in the H₂O masers (Alcolea, Menten, Moran, & Reid 1993).

Why does the Doppler velocity change over the eight years between our two VLBI epochs? The possibility that structural changes have occurred in the feature was mentioned above. A second possibility is that these masers, unlike typical HII region masers, are likely to occur in a strongly accelerated region, the region between the terminus of the H₂O outflow and the dense ambient molecular cloud. If this is the case, it would not be unreasonable to find a change of 0.5 km s^{-1} in Doppler velocity between the two epochs.

Bloemhof, Reid & Moran (1992) note a flux density calibration uncertainty of about 20% in the VLBI data. Since this can not account for the difference among the three epochs, we conclude that this feature is variable.

3. Discussion

3.1. OH Masers Associated with the TW protostar

The OH maser features described in this paper are not associated with the UCHII region in W3 OH, where strong OH and class II CH_3OH maser emission is found (Reid et al. 1980; Bloemhof, Reid, & Moran 1992; Menten 1991; Moscadelli, Menten, Walmsley, & Reid 1999). Instead, as seen in Fig. 2 their positions, and the 1665 MHz feature proper motion, suggest an association with the TW object and its intense H_2O masers (Alcolea, Menten, Moran, & Reid 1993). The association of some OH masers in W3 OH with the TW object and its H_2O masers suggests that some interstellar OH masers that are offset from HII regions may be associated with protostellar outflows and very young stars which have yet to, or may never, ionize their surroundings.

The TW object is thought to be a newly formed or forming massive star (Turner & Welch 1984; Wilner, Reid, & Menten 1999) or stars (Wyrowski, Schilke, Walmsley, & Menten 1999), which have yet to ionize their placental material. The “hot core” nature of the TW object was established by observations of high excitation NH_3 (5,5) inversion lines, which yield an NH_3 rotation temperature of 180 K (Mauersberger, Wilson, & Walmsley 1986). While the TW object shows no detectable thermal bremsstrahlung, surprisingly, it is a source of synchrotron emission (Reid et al. 1995). When imaged at high resolution (0."2) and sensitivity (10 μJy rms) with the VLA, the synchrotron source appears as an elongated, wiggling, double-sided jet (Wilner, Reid, & Menten 1999). The predominantly east–west orientation of the synchrotron jet matches both the spatial distribution and proper motions of the H_2O masers. Also, the center of the synchrotron jet lies, within measurement uncertainties of 0."1, at the center of expansion of the H_2O masers (Alcolea, Menten, Moran, & Reid 1993).

Comparison of the positions and velocities of the TW source OH masers with the dust continuum and molecular line emission mapped by Wyrowski et al. (1997) and Wyrowski, Schilke, Walmsley, & Menten (1999) also indicates a very close correspondence. Both the 1665 and the 1667 MHz masers project on the edges of the dust continuum/molecular emission. The thermally excited molecular gas displays an apparent shift in velocity across the source, with v_{LSR} changing from about -52 km s^{-1} at the eastern edge to about -45 km s^{-1} at the western edge. This trend of velocity increasing from east to west is consistent with our OH maser velocities.

The arrangement of the OH masers at, or just beyond, the ends of the H_2O maser outflow is noteworthy. One possible explanation for this arrangement is that the H_2O molecules in the outflow are dissociated at the extremities of the source, producing OH molecules with sufficient density to yield detectable maser emission. H_2O masers are estimated to require

H_2 densities between 10^8 and 10^{10} cm^{-3} , whereas OH masers require densities between 10^5 and 10^7 cm^{-3} (Elitzur (1992) and references therein). The upper limits to the H_2 densities are established by collisional thermalization of the level populations and quenching of the population inversions. The lower limits arise from estimates of the minimum column density necessary to achieve strong maser amplification over reasonable path lengths. Therefore, the transition from H_2O to OH masers in a source like the TW object suggests a rapid decrease in density with distance and a sharp boundary for the elongated region of H_2O maser activity.

Confirmation of a sharp molecular boundary comes from mm-wavelength observations of dust continuum emission. The molecular column density inside of the OH masers in the TW object, inferred from the dust continuum, of $N_{\text{H}_2} \sim 3 \times 10^{24} \text{ cm}^{-2}$ indicates a volume density of $n_{\text{H}_2} \sim 10^8 \text{ cm}^{-3}$, assuming a line of sight path length of 0.01 pc (P. Schilke, pers. comm.). The relatively sharp boundary of the dust continuum emission suggests that the molecular density must drop by a factor of 10 or more within a projected distance of about 0.005 pc at the edge of the source. Possibly, when molecular densities fall below $\sim 10^7 \text{ cm}^{-3}$, interstellar ultraviolet photons can dissociate H_2O molecules and create OH radicals.

3.2. Comparison to Other Regions: Shock Chemistry

While most interstellar OH masers do not show evidence of strong outflows, there is conclusive evidence that H_2O masers in regions of massive star formation partake in strong outflows from both 1) the large radial velocities observed, exceeding $\pm 100 \text{ km s}^{-1}$ in Orion-KL (Genzel, Reid, Moran, & Downes 1981a), and 2) the proper motions measured there and in W51 Main (Genzel et al. 1981b), Sgr B2 (Reid et al. 1988), W49 N (Gwinn, Moran, & Reid 1992). Of course the H_2O masers in W3 OH-TW also show a clear bipolar flow (Alcolea, Menten, Moran, & Reid 1993), and the $\sim 50 \text{ km s}^{-1}$ proper motion of one of the OH masers from the TW object suggests that at least some of the weak OH masers in the new class introduced by Gaume & Mutel (1987) are also associated with strong outflows.

The shock chemistry calculations of Neufeld & Dalgarno (1989) show that behind the front of a dissociative (“J”) shock of velocity 80 km s^{-1} , OH re-forms at a high abundance approaching $[\text{OH}/\text{H}] \approx 10^{-5}$, while the H_2O abundance is about an order of magnitude lower. In contrast, behind a non-dissociative (“C”) shock almost all the oxygen becomes tied up in H_2O (e.g., Draine, Roberge, & Dalgarno 1983). The velocities in most H_2O -emitting outflows are lower than 50 km s^{-1} , indicating non-dissociative shocks (in whose aftermath conditions are very conducive for pumping H_2O masers; Elitzur (1992)). This might explain why the H_2O masers are always much more powerful (by up to more than 4 orders of magnitude)

than the OH masers in W3 OH-TW (and Orion-KL as discussed below). Alternatively, as mentioned above, the densities necessary for 22 GHz H₂O maser action are two orders of magnitude higher than the values usually invoked for OH masers, and the OH maser emission should be quenched at these densities.

The masers associated with the TW object and those associated with source-I in the Orion-KL region (Menten & Reid 1995) have definite similarities. Both are associated with strong outflows. They have weak (or undetectable) thermal continuum emission at radio wavelengths and no clear, direct IR detections. Also both have strong H₂O and weaker OH masers. If the OH masers in Orion-KL and W3 OH-TW have a similar origin, then why is it that toward Orion-KL Johnston, Migenes, & Norris (1989) find many dozen features in the 1665 MHz (and about 2 dozen in the 1612 MHz) OH line, while we detect only one each in the 1665 and 1667 MHz lines (and none in the 1612 MHz line) toward W3 OH-TW? Given our (4 σ) detection limit of roughly 0.1 Jy, we would detect a 2.5 Jy strong feature in Orion put at the roughly 5 times larger distance of W3OH. Thus, we would detect 25 of the Johnston et al. 1665 MHz features, many of them barely, and one of their 1612 MHz features. Although no strong correlation between H₂O and OH luminosity seems to have been established yet, we note that the maser luminosity in both species is about an order of magnitude greater in Orion-KL than W3 OH-TW, as is the case for the infrared luminosity in both regions. This makes the paucity of OH features observed toward W3 OH-TW compared to Orion-KL understandable.

3.3. OH Maser/UCHII Region Association

In regions of massive star formation, one often finds interstellar OH masers. The traditional view is that interstellar hydroxyl masers (and class II methanol masers) form in the slowly expanding (3 to 10 km s⁻¹), dense ($\lesssim 10^7$ cm⁻³), and warm (≈ 150 K) molecular layers driven by the expanding UCHII region (e.g., Elitzur & de Jong (1978); Cesaroni & Walmsley (1991); Menten (1997)), where the OH is likely formed by photo-dissociation of H₂O. Since the strongest OH sources are generally associated with UCHII regions, most researchers have concluded that OH masers are probably associated with massive OB-type (ionizing) stars. However, it may well be that the “traditional” OH–UCHII region association picture emerged due to a selection effect, caused by the fact that earlier searches for OH masers were conducted predominantly toward HII regions. At least three surveys suggest that this is indeed the case.

In Argon, Reid, & Menten (2000), we selected for observation interstellar OH masers whose declinations were above -45° and peak flux densities were stronger than 1 Jy in both

circular polarizations in at least one OH main-line transition. We observed 91 OH masers and noted that our sample was at least 80% complete. Towards each of the observed OH maser regions, we also looked for 8.4 GHz continuum emission detectable above a noise level of ≈ 0.15 mJy beam $^{-1}$. The Maser–UCHII region association was judged by analogy to W3 OH. In W3 OH, the OH masers closer than 3" to the center of the brightest 8.4 GHz continuum emission ($\approx 2"$ from the edge) appear to be associated with the UCHII region, while the OH masers farther away (i.e., those we have associated with the TW source) are not. At a distance of 2.2 kpc (Humphreys 1978) to W3 OH, 2" corresponds to 0.02 pc. We then examined all sources in the Argon, Reid, & Menten (2000) survey and found that in only 49 of the 91 maser fields (54%) were *any* of the OH masers closer than 0.02 pc to the edge of an UCHII region.

In another recent survey, Forster & Caswell (2000) presented a search for 8.5 GHz radio continuum emission toward 45 sites of OH and H₂O maser emission with Galactic longitudes in the range 352.[°]52 to 24.[°]79. Only toward 17 of them did they find continuum emission above a detection threshold of approximately 0.5 mJy beam $^{-1}$. (At this frequency, according to Forster & Caswell (2000), an ionization-bounded, optically thin, HII region produced by a ZAMS star of spectral type B1 at a distance of 5 kpc is 1 mJy and would have been detected.) If one considers only the OH maser regions and uses the maser-continuum association criterion described above, one finds that only 16 of the 26 (62%) regions that contain OH masers have associated continuum emission.

Finally, Gaume & Mutel (1987) studied the ground state OH maser and 15 GHz continuum emission associated with 11 regions of star formation, demanding only that the 1720 MHz OH transition be present when selecting regions for study. They noted that 75 – 80% of the maser clusters within their 11 regions appeared to be closely associated with HII emission. Detection limits (rms noise levels) varied widely from source to source but typically were in the range of a 0.3 mJy beam $^{-1}$ to 3 mJy beam $^{-1}$. Although this percentage is not directly comparable to the percentages from the two previous surveys, since we did not attempt to subdivide maser regions into maser clumps when discussing those surveys, it does strengthen the argument that many OH masers have no associated continuum. Gaume & Mutel (1987) grouped these unassociated masers into a separate “class” and noted that they tended to be much weaker than other OH masers.

How does one explain the presence of OH masers with no associated continuum? At least two possibilities come to mind. First, the masers may be associated with a very young HII region that is currently below the detection limit because of its small size. While one might expect this phase in the development of an UCHII region to be very brief, Keto (2002) show that the strong gravitational attraction of material very close to a massive star

can significantly extend the lifetime of this phase. In the future, these HII regions can be expected to grow larger and become detectable. An alternative possibility for the absence of an UCHII region near some OH masers is that these masers may be associated with a star that will never give rise to an HII region. The TW source and other outflow regions, for example, may contain a central star less massive than a B3 star and not produce sufficient ionizing photons to create a detectable UCHII region.

It is uncertain how many of the OH masers with no detected continuum emission are similar to the TW object masers. In general, OH masers associated with outflows can be expected to have weak features spanning tens of km s^{-1} in radial velocity. In the survey of Argon, Reid, & Menten (2000) $\approx 20\%$ of interstellar OH maser spectra have velocity spreads $\gtrsim 10 \text{ km s}^{-1}$ and $\approx 5\%$ have velocity spreads $\approx 30 \text{ km s}^{-1}$, the latter being inconsistent with the expansion velocity of a compact HII region. Unfortunately, it is possible that most surveys could have missed weak, high velocity, maser features owing to bandwidth and sensitivity limitations.

While the spread in radial velocity of the OH masers toward W3 OH is not large ($\approx 9 \text{ km s}^{-1}$), the observed proper motion of the 1665 MHz maser toward the TW source is very large, implying that the outflow in this source lies close to the plane of the sky. This is corroborated by the proper motions measured for the TW H₂O masers by Alcolea, Menten, Moran, & Reid (1993). This may not be a coincidence, since there may be a preferential orientation for observing detectable masers in a bipolar outflow. For outflows, the longest gain paths are likely to be perpendicular to the outflow axis. Thus, these masers may be strong only when the outflow axis is nearly perpendicular to our line of sight, and they would show small Doppler shifts from the systemic velocity. If this effect is important, then a significant fraction of the OH masers with no detected continuum emission could be associated with outflows.

4. Conclusions

During an interferometric survey of OH masers in star-forming regions, we detected weak OH maser emission associated with the Turner-Welch object, a very deeply embedded protostellar object. Using archival VLBI data, we were able to determine the proper motion of one of the maser features, which is of comparable magnitude and direction as the proper motions of the H₂O masers, which arise from a bipolar outflow centered on the TW object. While conventional wisdom associates OH masers with the slowly expanding molecular envelopes of ultracompact HII regions, we argue that the W3 OH/TW OH masers are part of a new class of OH masers that trace protostellar outflows. Another example of this class of

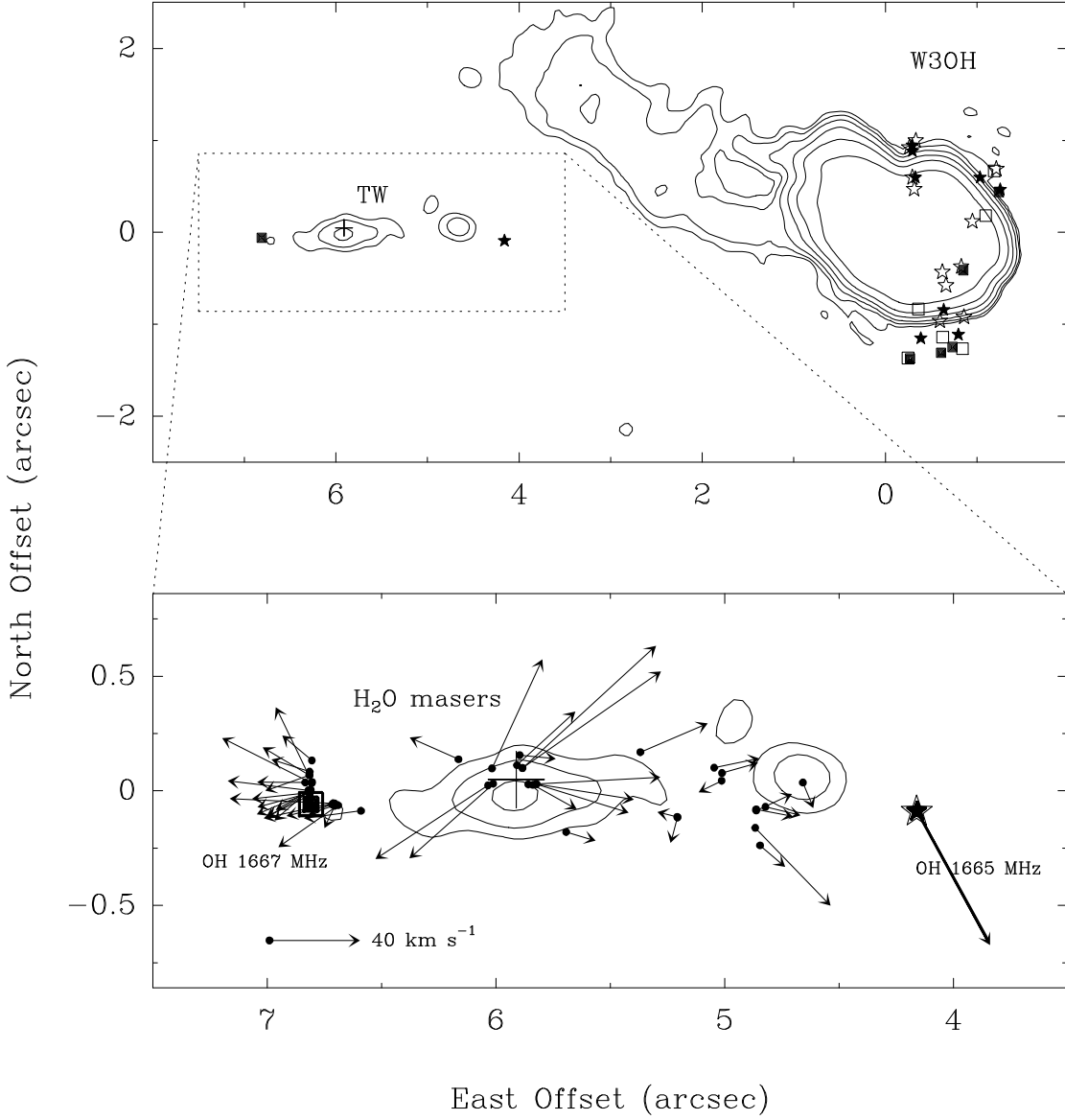


Fig. 2.— (Top panel) 1665 and 1667 MHz OH masers from Argon, Reid, & Menten (2000) and two “outlying” OH masers (this paper) superimposed on the 8.4 GHz VLA contour plot of Wilner et al. (1999). The “stars” represent 1665 MHz OH maser emission and the “squares” 1667 MHz OH maser emission. Open symbols are RCP and closed symbols LCP. ‘TW’ stands for the Turner-Welch object (Turner & Welch 1984). (Lower panel) H₂O and outlying OH maser emission near the Turner Welch object. Positions and proper motions of the H₂O masers are indicated by filled circles and light arrows, respectively (Alcolea *et al.* 1993) and the large cross marks the H₂O maser center of expansion determined by these authors. Positions of the OH masers are indicated by either a “star” or a “square” (this paper) and the single proper motion by a heavy arrow. The origin of coordinates corresponds to $\alpha_{B1950} = 02^h23^m16.^s499$, $\delta_{B1950} = 61^\circ38'57.''21$.

OH masers might be the Orion-KL/IRc 2/Source-I masers and, possibly, some of the sources mapped by Forster & Caswell (2000) in which OH and H₂O masers are coexistent and are offset from continuum emission.

The near spatial coincidence of OH and H₂O maser emission in outflow sources may be explained by OH production by photo-dissociation of H₂O by the interstellar radiation field. The densities required for H₂O maser action are roughly two orders of magnitude higher than those suitable for OH masers. This is consistent with the observation that the OH maser spots are located at the outer edges of the H₂O emission region. One important avenue of future research suggested by our results is high spatial resolution observations of this class of OH masers, since OH is an important chemical constituent of post-shock gas not otherwise observable with comparable resolution.

REFERENCES

Alcolea, J., Menten, K. M., Moran, J. M., & Reid, M. J. 1993, in *Astrophysical Masers*, ed. A. W. Clegg & G. E. Nedoluha (Springer Verlag: Berlin), 225

Argon, A. L., Reid, M. J., & Menten, K. M. 2000, *ApJS*, 129, 159

Bloemhof, E. E., Reid, M. J., & Moran, J. M. 1992, *ApJ*, 397, 500

Cesaroni, R. & Walmsley, C. M. 1991, *A&A*, 241, 537

Draine, B. T., Roberge, W. G., & Dalgarno, A. 1983, *ApJ*, 264, 485

Elitzur, M. 1992, *ARA&A*, 30, 75

Elitzur, M. & de Jong, T. 1978, *A&A*, 67, 323

Forster, J. R. & Caswell, J. L. 2000, *ApJ*, 530, 371

Garcia-Barreto, J. A., Burke, B. F., Reid, M. J., Moran, J. M., Haschick, A. D., & Schilizzi, R. T. 1988, *ApJ*, 326, 954

Gaume, R. A. & Mutel, R. L. 1987, *ApJS*, 65, 193

Genzel, R., Reid, M. J., Moran, J. M., & Downes, D. 1981, *ApJ*, 244, 884

Genzel, R. et al. 1981, *ApJ*, 247, 1039

Gwinn, C. R., Moran, J. M., & Reid, M. J. 1992, *ApJ*, 393, 149

Humphreys, R. M. 1978, *ApJS*, 38, 309

Johnston, K. J., Migenes, V., & Norris, R. P. 1989, *ApJ*, 341, 847

Keto, E. 2002, *ApJ*, 580, 980

Mauersberger, R., Wilson, T. L., & Walmsley, C. M. 1986, *A&A*, 166, L26

Menten, K. M. 1991, in *ASP Conf. Proc. 16, Atoms, Ions and Molecules: New Results in Spectral Line Astrophysics*, ed. A. D. Haschick & P. T. P. Ho (ASP: San Francisco), 119

Menten, K. M. 1997, in *IAU Symp. 178, Molecules in Astrophysics: Probes & Processes*, ed. E. van Dishoeck (Kluwer: Dordrecht), 163

Menten, K. M. & Reid, M. J. 1995, *ApJ*, 445, L157

Moscadelli, L., Menten, K. M., Walmsley, C. M., & Reid, M. J. 1999, *ApJ*, 519, 244

Neufeld, D. A. & Dalgarno, A. 1989, *ApJ*, 340, 869

Reid, M. J., Argon, A. L., Masson, C. R., Menten, K. M., & Moran, J. M. 1995, *ApJ*, 443, 238

Reid, M. J., Haschick, A. D., Burke, B. F., Moran, J. M., Johnston, K. J., & Swenson, G. W. 1980, *ApJ*, 239, 89

Reid, M. J., Schneps, M. H., Moran, J. M., Gwinn, C. R., Genzel, R., Downes, D., & Roennaeng, B. 1988, *ApJ*, 330, 809

Turner, J. L. & Welch, W. J. 1984, *ApJ*, 287, L81

Wilner, D. J., Reid, M. J., & Menten, K. M. 1999, *ApJ*, 513, 775

Wyrowski, F., Hofner, P., Schilke, P., Walmsley, C. M., Wilner, D. J., & Wink, J. E. 1997, *A&A*, 320, L17

Wyrowski, F., Schilke, P., Walmsley, C. M., & Menten, K. M. 1999, *ApJ*, 514, L43